30th International North Sea Flow Measurement Workshop
23 – 26 October 2012

Assessment of Particle Erosion in Coriolis Meters

Mark J. Bell, Emerson Process Management
Mark MacLeod, NEL

1 INTRODUCTION

This paper describes a project in which Computational Fluid Dynamics (CFD) and Finite Element Analysis (FEA) were used to assess the effect of particulate erosion in two of Emerson's Micro Motion Coriolis flow meters, a 3 inch dual "u" shaped meter (CMF300), and a 3 inch dual slightly curved tube meter (F300).

These flow meters have been used in a wide range of applications, in some instances to measure particle-laden fluids. Occasionally flow meters are returned due to particulate erosion damage, although this is a rare occurrence. The aim of this work was to develop a better understanding of particle erosion in Coriolis meters over a wide range of operational conditions.

The erosion analysis was carried out using CFD (Computational Fluid Dynamics). The pattern and magnitude of erosion was investigated. The erosion results were then coupled to a FEA solver to investigate the structural and flow measurement impact of erosion on the Coriolis meters.

2 LITERATURE SUMMARY

Erosion is an important factor determining the lifespan of any component when the fluid flowing through the component contains solid particles. Particulate erosion is the process of metal removal by solid particle impact. This is a complex process with many different factors involved. Parameters that influence erosion rates range from the properties of the fluid (flow rate, velocity, and viscosity), the properties of the sand, the properties of the target material, and the geometry of the component or pipe work in question. The result of this complexity is that small variations in certain parameters can cause significant differences in erosion rates and erosion locations. McLaury et al. [1] looks at some of these parameters and how they affect erosion rates.

Pipe bends are an essential part of any piping system and are prone to significant erosion damage. Toda et al. [2] observed that when particles encounter a bend, the particles do not follow the fluid streamlines but are forced along the outer wall of the bend. Particle size and fluid properties can affect the flow patterns of particles. Okita [3] investigated the effect of viscosity and sand size on erosion measurement and prediction. This work showed lower viscosities produce greater erosion rates and also showed that viscosity has little effect on particles greater than 150 microns diameter.

Another factor that influences erosion in bends is the upstream flow profile. The upstream flow profile can be affected by upstream bends or other fixtures. The effect of combining elbows will affect the erosion pattern and magnitude. Schallert et al. [4] shows that combining elbows in series can change the expected erosion locations and rates. Erosion is generally higher in fixtures downstream of other fixtures. Barton et al. [5] noted how the presence of upstream flow meters increased the erosion rate of a downstream bend.

Smaller particles are generally perceived as being less erosive although this is still a subject of research. Small particles have less momentum; they are more easily deflected by fluid drag forces and hence tend to impact walls at lower angles and velocities. However, they can also be more easily entrained behind backward-facing steps and hence scouring effects may be more common for smaller particles. Misra and Finnie [6] showed that particles smaller than 100 microns are less damaging (Figure 1). This effect occurs for a range of metals in both erosion and abrasions tests and appears to be associated with the "micro-machining" process of material removal rather than particle and fluid dynamic effects.

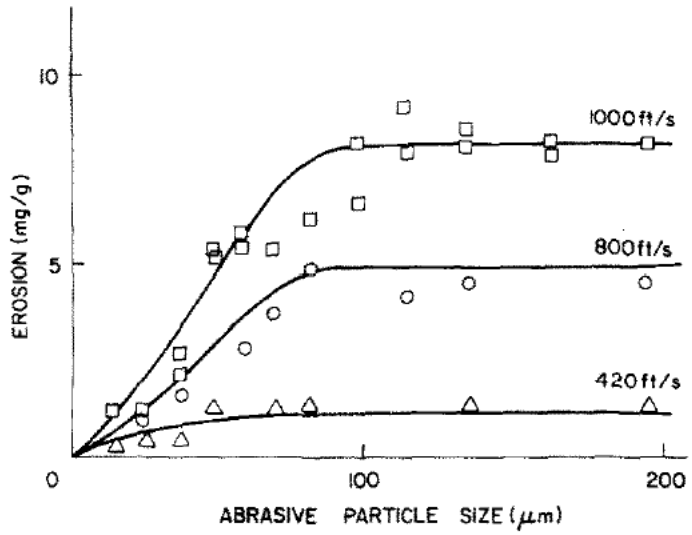

Figure 1 The effect of particle size on the erosion rate of 11% Cr steel [6]

A number of guidance documents are available to manage sand erosion problems. DNV RPO501[7] is one of the most comprehensive available guidelines for the assessment of erosive wear in piping systems associated with sand production in the oil and gas industry. These guidelines include calculations that can give numerical predictions for erosion in standard pipe fixtures such as straight pipes, elbows, welded joints, reducers and blind tees.

3 SIMULATION METHOD AND PARAMETERS

The CFD simulations of the F300 and CMF300 meters consisted of some water-sand flow cases and some gas-sand flow cases. Certain properties were varied to investigate their effects on erosion. The flow through the flow meters was modelled using Fluent 13 CFD software [8],
Figure 2. The CMF300 has a tube diameter of 44.7 mm while the F300 has a tube diameter of 40.2 mm. The beta ratio for the CMF300 is 0.81 to a DN80 pipe and the F300 is 0.73 to the same DN80 pipe. This difference in diameters provides meters that have similar pressure drop at the same flow rate.

When a particle impacted onto a wall the damage this caused was calculated using the following equation [9]:

$$\dot{E} = C_{unit}\dot{m}_P.K.U_P^n.F(\alpha) \qquad (1)$$

In which:

E	is the erosion rate (mm/kg of sand passing through the pipe work)
C_{unit}	is a factor to convert the erosion rate to mm/kg
m_p	is the mass flow rate of sand impacting the region in question (kg/s)
U_P	is the particle impact velocity (m/s)
α	is the impact angle
F(α)	is a function that accounts for the variation of erosion caused by differing impact angles.

In this study values of K, n and the F(α) were chosen to represent generic “steel grade materials” based on values given in DNV RP0501 [7].

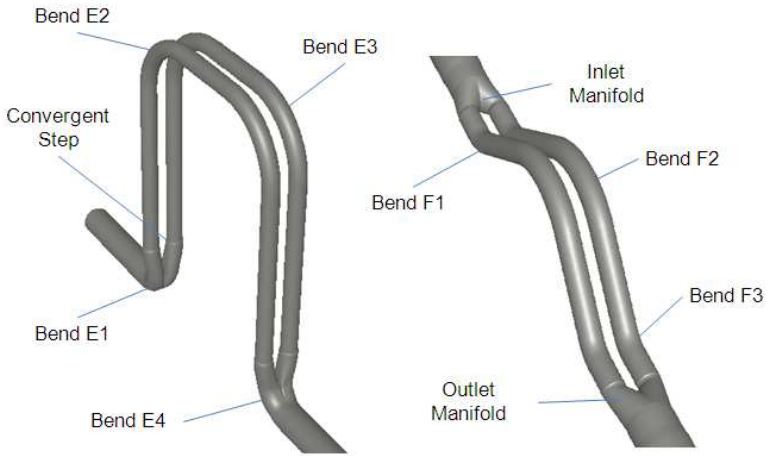

Figure 2 CMF300 meter on the left and F300 meter on the right

The modelled cases were split into four batches of runs. Each batch of runs was used to assess the sensitivity of erosion to one selected variable parameter as noted in Table 1. These parameters included; fluid velocity, particle diameter, fluid viscosity and upstream installation effects.

Table 1 – Analyses Batches (variable parameter in bold)

Batch	Fluid	inlet velocity* m/s	Density kg/m3	Viscosity cp	Particle Diameter µm	Upstream Bend
1	Water	**2 - 10**	1000	1	150	No
	Gas	**10 - 50**	20	0.018	150	No
2	Water	10	1000	1	**50 - 300**	No
3	Water	10	1000	**1 - 1000**	150	No
4	Water	10	1000	1	150	**Yes**

*Inlet velocity defined by velocity at the inlet of the flow meter not the velocity in the tubes.

For each case the erosion was also calculated using the semi-empirical equation developed by DNV [7].

$$\dot{E}_L = \frac{K \times F(\alpha) \times \sin\alpha \times U_p^n}{\rho_t \times A_{pipe}} \times G \times C_1 \times C_{unit} \qquad (2)$$

$\dot{E}_L$ = Erosion rate (mm/kg)
K = Material Constant
$F(\alpha)$ = Function characterizing ductility of material
α = Impact angle of particles hitting wall
U_p = Particle impact velocity (m/s)
n = Velocity exponent
ρ_t = Density of target material (kg/m^3)
A_{pipe} = Cross-sectional area of pipe (m^2)
G = Correction function for the particle diameter
C_1 = Model/geometry factor
C_{unit} = Unit conversion to mm/kg

This equation is for erosion in a 90° 1.5D bend. This is used to estimate the erosion in the bends of the CMF300 and F300 meters. It is a simplified approach that doesn't take into account the presence of upstream bends.

4 RESULTS

4.1 Batch 1 Erosion Results (Baseline - 150 µm Particles)

The following plots show the erosion contours for selected cases in terms of millimetres of erosion per kilogram of particles passing though the meter (mm/kg). The flow direction is indicated by arrows.

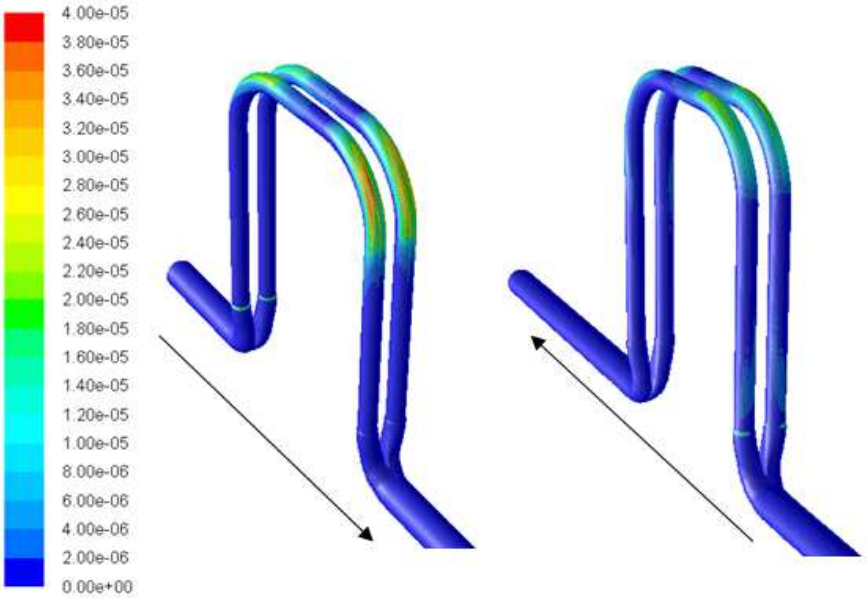

Figure 3 Erosion contour plot for water flow - Case 1-5 (mm/kg)

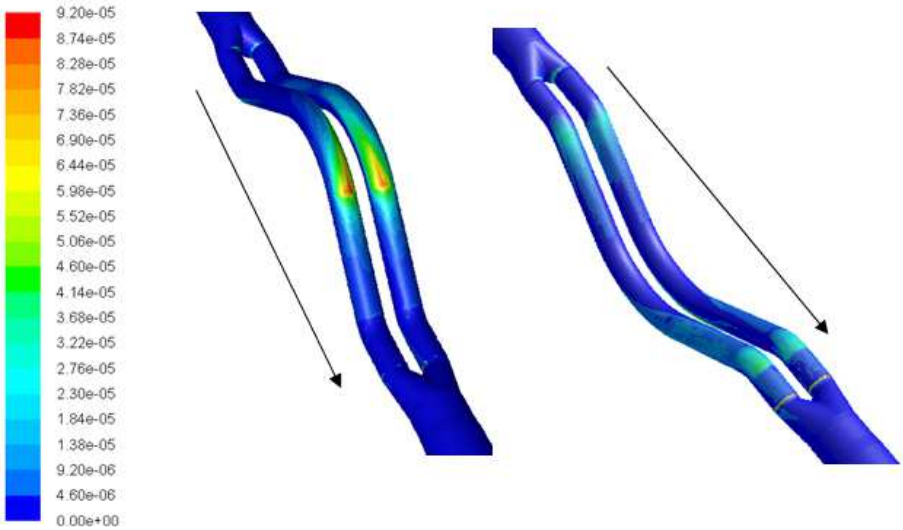

Figure 4 Erosion contour plot for water flow - Case 1-10 (mm/kg)

Figure 3 is an erosion contour plot for the CMF300 meter, case 1-5. The erosion peaks at 4e-5 mm/kg and is located in bend E3. The fluid velocity in the tubes is higher than the fluid velocity at the inlet due to the differences in cross-sectional area thus resulting in higher erosion rates around bend E2 and E3. The sand particles tend to follow the outside of the bend due to their momentum hence the erosion scars on the outer surface of the bends. It is also noted that when there are multiple bends in a geometry, the downstream bend, generally speaking, will experience higher erosion rates. Rings of slightly increased erosion are found on the flow tubes near the splitter, where cross-sectional area is slightly reduced due to weld penetration. These locations are where the flow tubes are welded to the manifold during manufacturing.

The erosion in the F300 meter, case 1-10, peaks at 9.2e-5 mm/kg (Figure 4). The maximum erosion location is found on the outside of bend F2 slightly downstream of the bend. This is again consistent with the particles impacting the outer wall of the bend as they are forced to the outside because of their momentum. Note that in comparing the two figures, the F300 erosion rate is more than two times the CMF300 rate; a result that was not expected. This difference is due to the increase in flow velocity in the flow tubes and the fact that more particles strike the tube wall at 45 degrees.

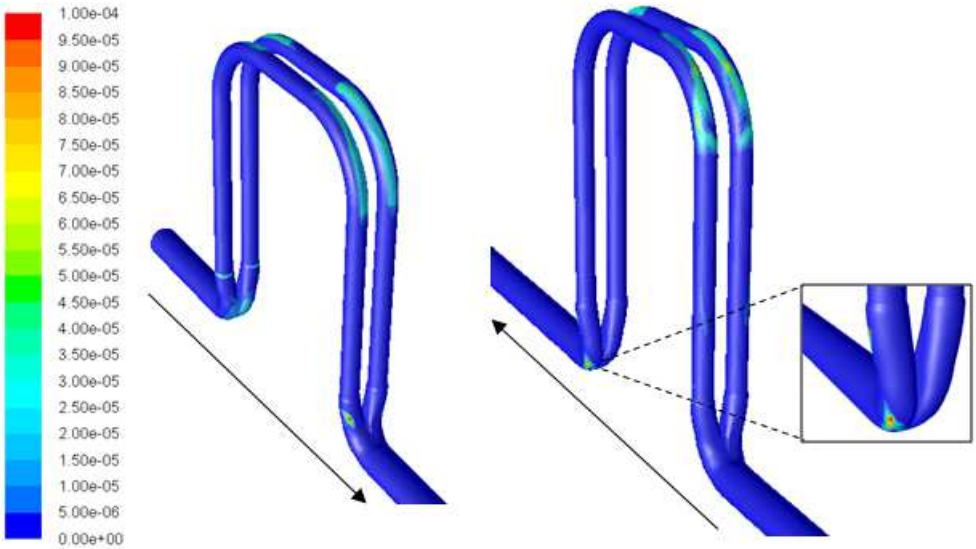

Figure 5 Erosion contour plot for gas flow - Case 1-11 (mm/kg)

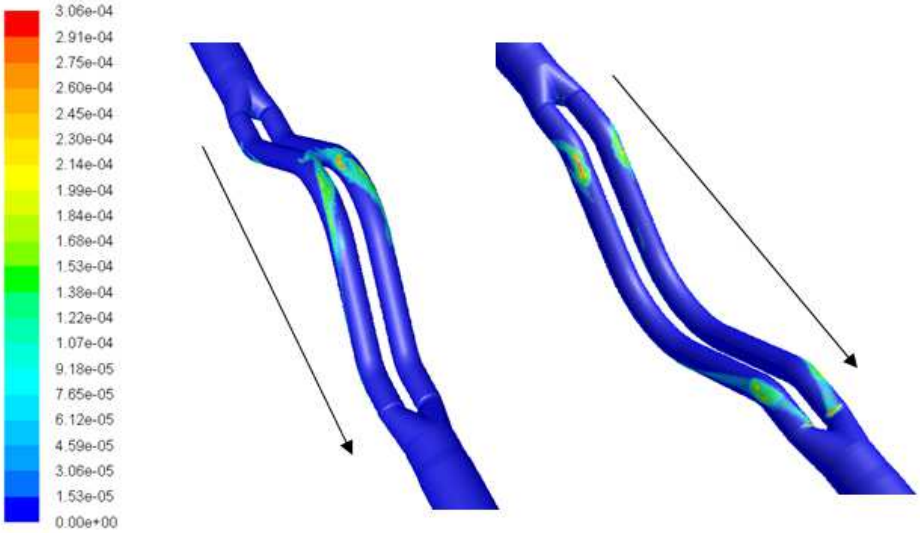

Figure 6 Erosion contour plot for gas flow - Case 1-14 (mm/kg)

The erosion in the CMF300 gas flow case, Figure 5, peaks at 1e-4 mm/kg and is located in bend E4. The erosion in the gas flow cases manifests itself in small erosion hot spots rather than the larger erosion scars as seen in water flow. Gas flows tend to produce more concentrated streams of particles that produce erosion hot spots.

A peak erosion rate of 3.06e-4 mm/kg is predicted for the F300 meter, located in bends F1, F2 and also the outlet manifold (Figure 6). However, it is noted that the erosion in the outlet manifold is due to a step in the geometry at the location of the tube to manifold welds. It is likely that the step will erode into a smoother face and the local erosion rate will reduce over time.

The remaining erosion results for batch 1 are plotted in Figures 7 and 8 which show the relationship between erosion and fluid velocity.

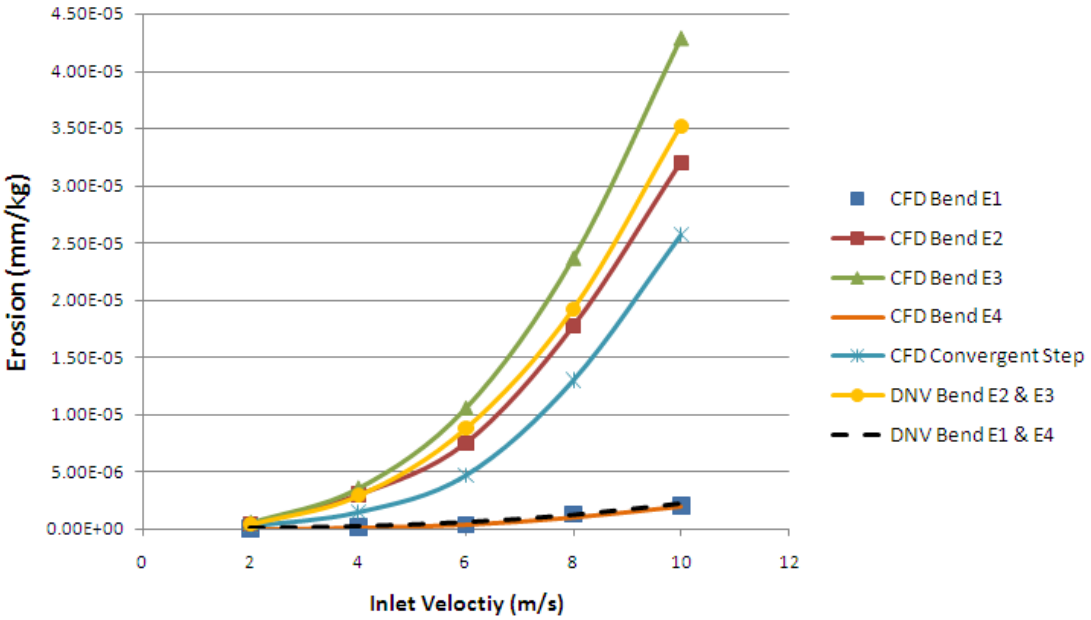

Figure 7 CMF300 Erosion rate variation with inlet velocity in water flow

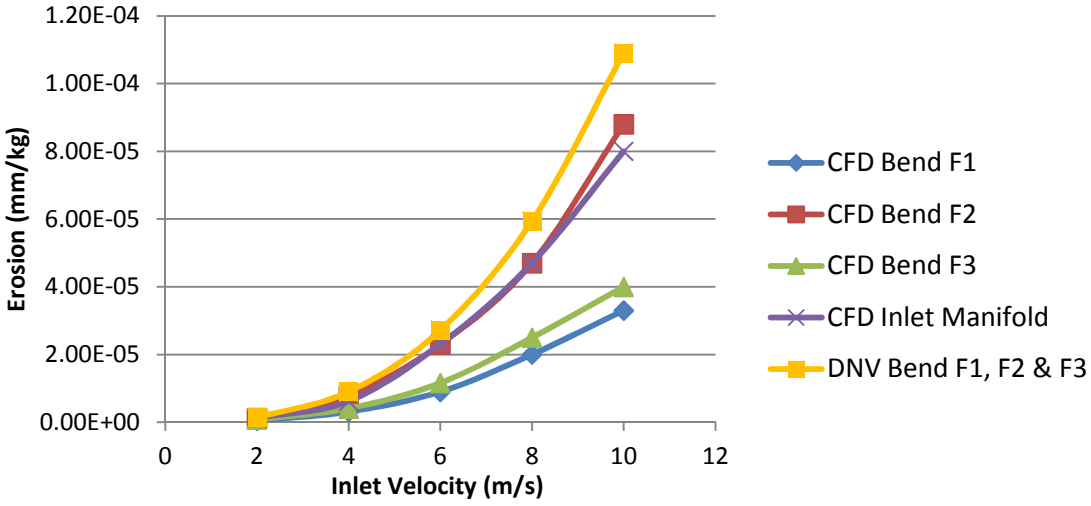

Figure 8 F300 Erosion rate variation with inlet velocity in water flow

The graphs show expected trends with erosion increasing substantially as velocity is increased. Erosion is roughly proportional to the mean flow velocity to the power of 2.6. The DNV RPO501 equation results show a good agreement with the CFD results given that erosion predictions are usually only accurate to within an order of magnitude.

In Figure 7 the DNV RPO501 results are lower than the CFD predicted results for bend E3. This may be because the DNV RPO501 calculation does not take into account the upstream bend which causes increased erosion.

In Figure 8 the DNV RPO501 results are higher than the CFD results. This is due to the geometry of the bends. The DNV RPO501 calculation assumes a 90° bend but the bends in the F300 meter are less than 90° thus resulting in lower erosion rates.

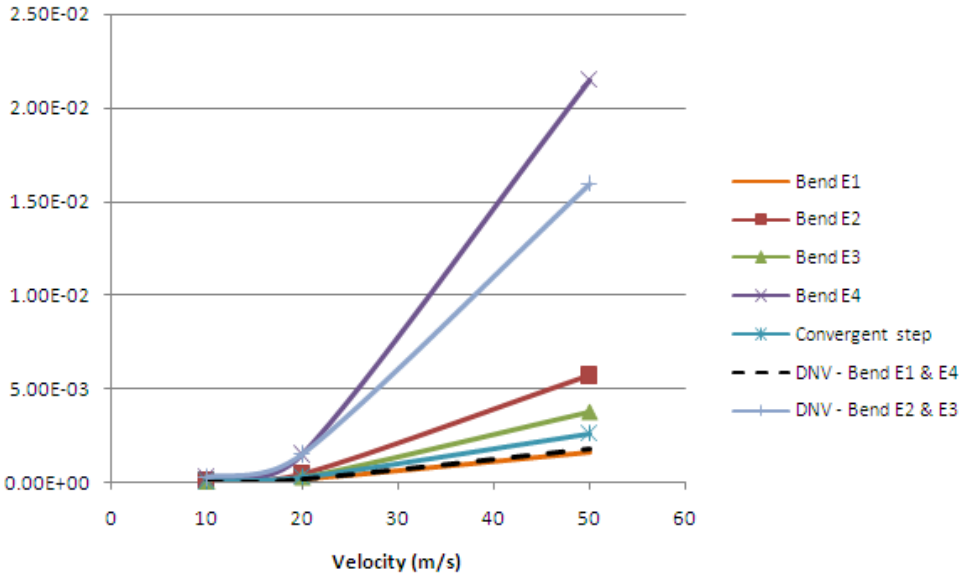

Figure 9 CMF300 Erosion rate variation with inlet velocity in gas flow

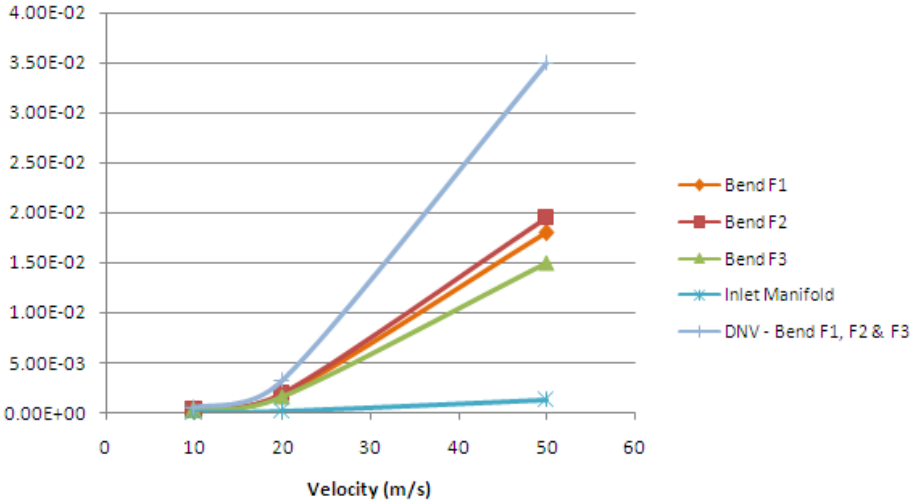

Figure 10 F300 Erosion rate variation with inlet velocity in gas flow

Figure 9 and Figure 10 show that the general erosion trends in gas flow are, for the most part, similar to water flow cases. The exception is the high erosion values in bend E4, Figure 9, where the erosion is significantly higher than elsewhere in the meter. The multiple upstream bends result in an accelerated erosion rate in bend E4. The DNV RPO501 equation, which does not take into account upstream bends, underestimates the erosion in bend E4 by a factor of 10. DNV RPO501 bend E2 & E3 values are closer estimates of the CFD bend E4 values. Therefore, DNV RPO501 bend E2 and E3 values should be used as estimates for all bends.

In the F300 meter, Figure 10, the DNV RPO501 equation tends to over-predict the CFD results as was evident in the water flow case.

4.2 Batch 2 Erosion Results (Particle Size Effects)

Figures 11 and 12 show the erosion rates varying with particle size in water flow.

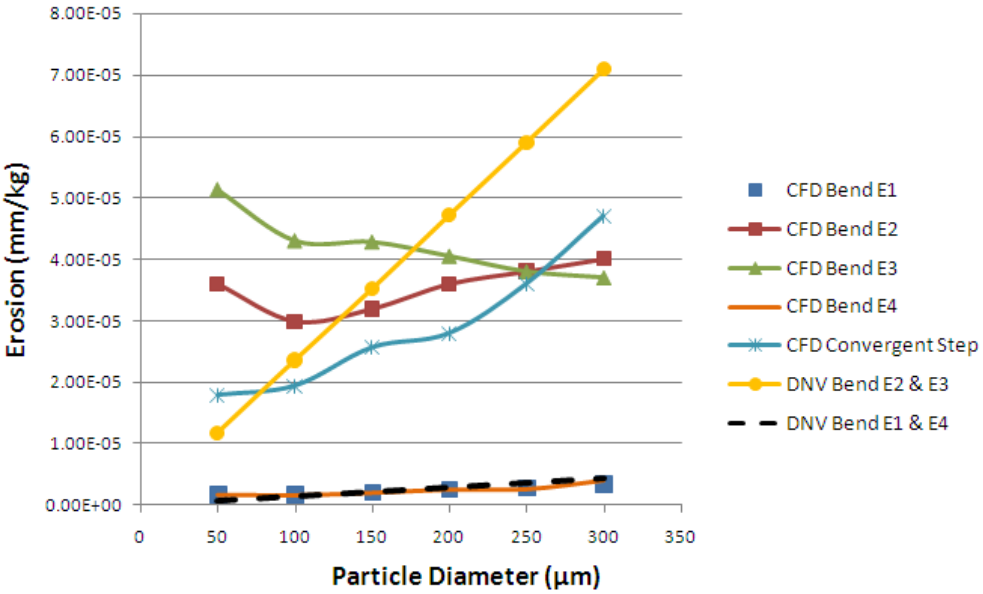

Figure 11 CMF300 Erosion rate variation with particle diameter

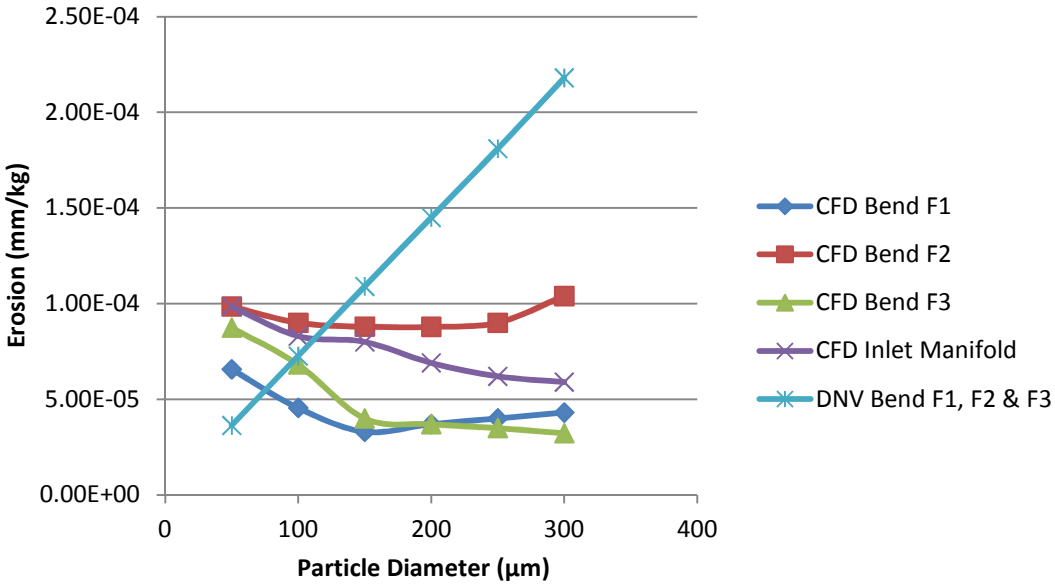

Figure 12 F300 Erosion rate variation with particle diameter

The particle size is having very little effect on the predicted erosion rate in most of the bends. Note that the size effect shown in Figure 1 is not represented in the CFD model, although this would only affect the 50 micron cases.

Bends E1 and E2, Figure 11, show a steady increase in erosion as particle size increases but the other bends in both geometries show little variation.

The DNV RPO501 calculation shows a linear relationship between erosion and particle size. It consistently predicts higher erosion rates than the CFD does for particle sizes greater than about 175 microns.

4.3 Batch 3 Erosions Results (Viscosity Effects)

The following contour plots and graphs show the relationship between erosion and viscosity in liquid flow. Note these are on a log scale for ease of comparison.

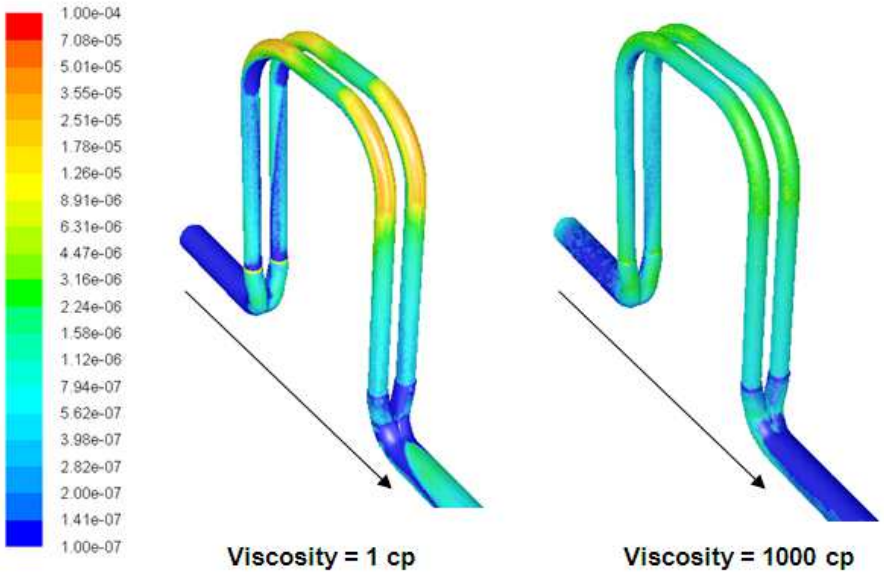

Figure 13 Log scale erosion contour plot - Case 1-5, left, and 3-3, right (mm/kg)

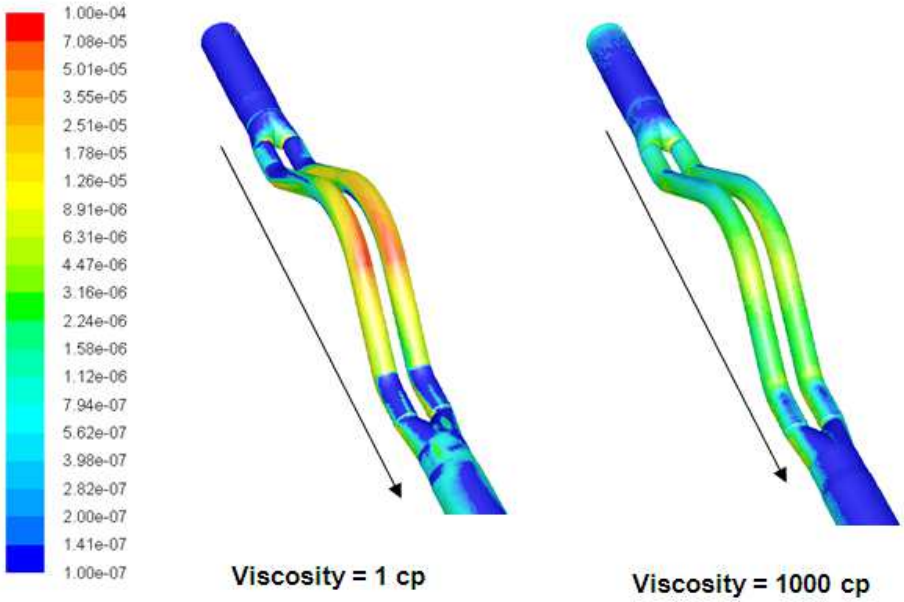

Figure 14 Log scale erosion contour plot - Case 1-10, left, and 3-6, right (mm/kg)

The contour plots above, Figure 13 and Figure 14, give a comparison between the two extreme ends of the modelled viscosity range. The 1000cp cases predict significantly smaller peak erosion rates than the 1cp cases - around one order of magnitude less. In general the erosion in the high viscosity cases is more evenly spread throughout the meter. The location of the peak erosion does not vary much with viscosity.

When viscosities are higher the viscous forces in the fluid are higher causing the particles tracks to be dominated by the fluid streamlines. This results in fewer particles impacting the walls and thus a lower predicted erosion rate.

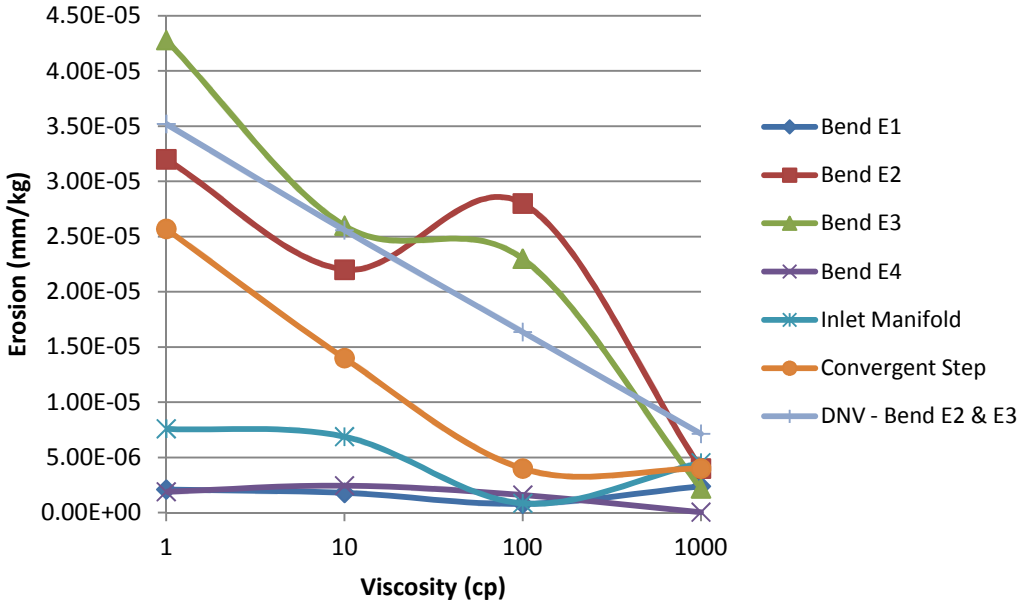

Figure 15 CMF300 Erosion rate varying with viscosity at inlet velocity = 10m/s

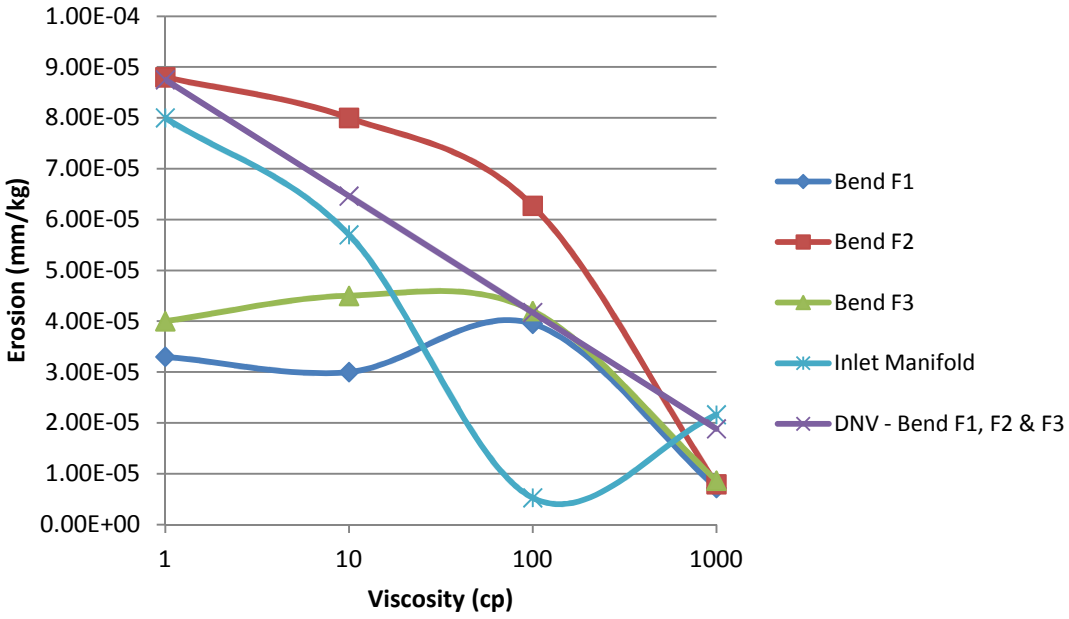

Figure 16 F300 Erosion rate varying with viscosity at inlet velocity = 10m/s

There is a general downwards trend in erosion as viscosity increases. The precise nature of the trends varies from graph to graph. The 100cp data points seem to deviate from the general trends in both graphs. Figure 17 shows Figure 15 re-plotted in terms of Reynolds number. It can be seen that the 100 cP data points correspond to the laminar-turbulent transitional flow regime. The peculiar 100 cP data points may be because the CFD model is less accurate in transitional flow.

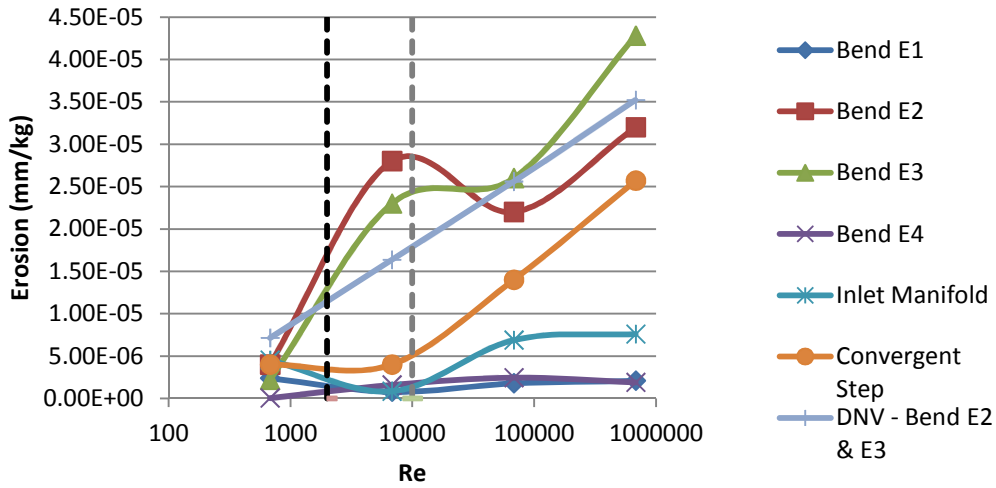

Figure 17 CMF300 erosion rate varying with Reynolds number at inlet velocity = 10m/s

The DNV RPO501 results, in Figure 15 and 16 show a linear reduction in erosion rate as viscosity increases. In each case the DNV RPO501 results give a reasonably good comparison with the CFD results.

4.4 Batch 4 Erosion Results (Effect of an Upstream Bend)

Figures 18 and 19 show the effect of placing a bend upstream of each Coriolis meter.

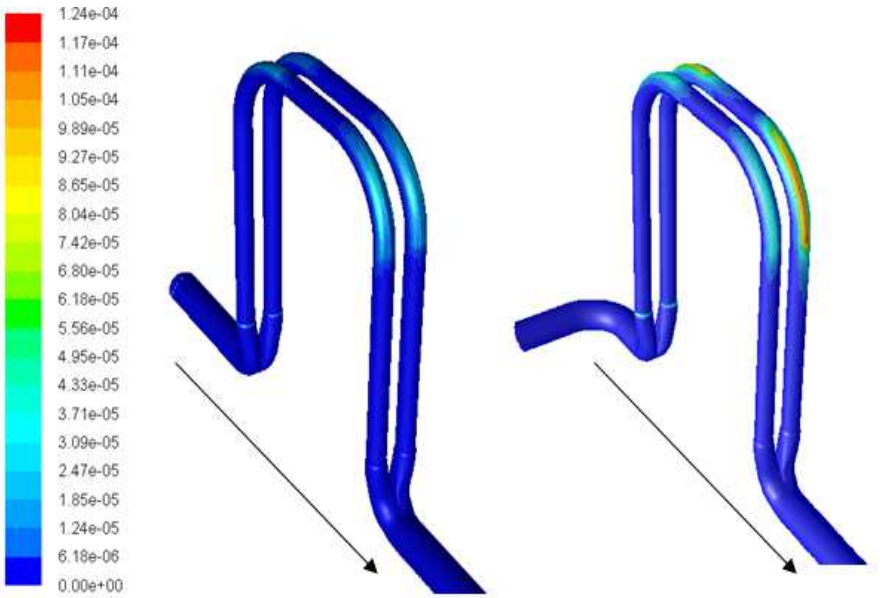

Figure 18 CMF300 erosion contour plot with upstream bend (mm/kg)

The presence of an upstream bend results in about four times more erosion than in the original model. This high erosion is only in one tube of the Coriolis meter. As was previously noted when particles approach a bend they are forced to the outside of the bend because of their momentum. If the inlet manifold is immediately downstream of a bend then the majority of particles will be forced down the outer tube resulting in high erosion in that tube. The presence of an upstream bend also induces more swirl into the flow which again can act to increase erosion in any downstream fixtures.

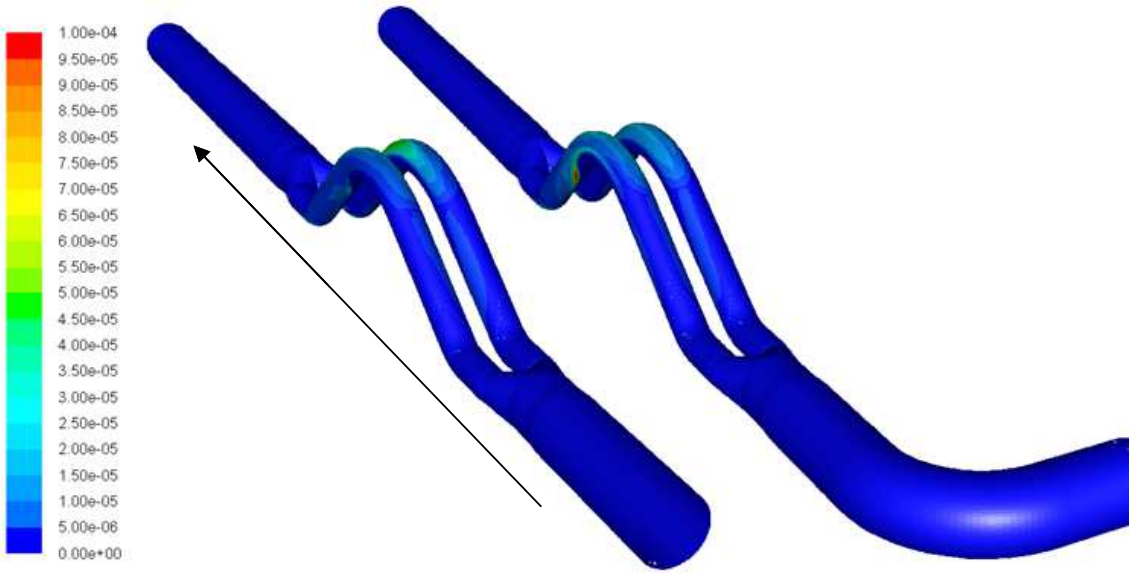

Figure 19 F300 erosion contour plot with upstream bend (mm/kg)

Figure 19 shows how the erosion pattern of the F300 meter changes with the inclusion of an upstream bend. The bend again induces added swirl into the flow resulting in a swirling erosion scar downstream of bend F2. It follows a similar trend to the CMF300 meter in that the erosion is concentrated in one of the tubes.

5 CFD EROSION PATTERN VALIDATION

Emerson provided failure reports of Coriolis meters which are believed to have failed due to particulate erosion. These failure reports indicate the location of failure and also provide wall thinning plots for the bends in the tubes of the meter.

In general the CFD-predicted erosion patterns in the tube bends matched those seen in the failure reports. However, the majority of actual failures occurred at the inlet manifold just as the flow splits into the two tubes. This may be due to small weld beads or steps in the geometry causing turbulent recirculation of particles. These geometrical features may not have been accurately represented in the CFD models. Also, the recirculating scour erosion that occurs behind steps in pipe bore in liquid flow is rarely captured using CFD.

The one failure report provided for liquid flow agrees reasonably well with the CFD predictions. The location of the failure is highlighted by a white arrow marked on the pipe. The geometry of this meter is similar to the CMF300 meter. Figure 5 shows that the CFD is predicting failure to occur in bend E3 which corresponds to the location with the minimum wall remaining in Figure 20.

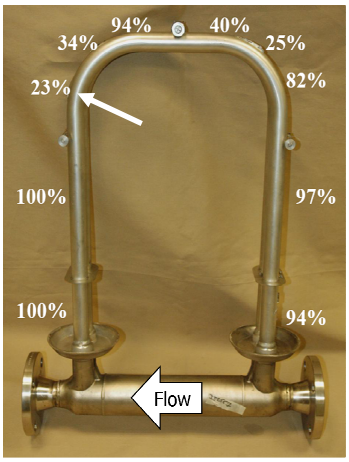

Figure 20 Liquid flow erosion report (% shows amount of wall remaining)

6 CORIOLIS BASICS AND EFFECTS FROM EROSION

A Coriolis meter is a flow measurement device that imparts vibration on the fluid and the response of the fluid on the vibrating element is used to measure mass flow and density of the fluid directly. In addition, these two primary variables are used to calculate volume flow. Since the vibration properties of steel change with temperature, a resistive temperature device (RTD) is used to measure and compensate for changes in temperature. From a single device, four variables are provided; mass flow, volume flow, density, and temperature. Coriolis meters have been available commercially for 35 years and continue to gain industry acceptance for liquid measurement, gas measurement, and also in erosive service (produced liquids, cement, mud, lime slurries, etc).

A schematic of a dual tube Coriolis meter is shown below. In this arrangement, flow enters the meter at the inlet, flow is split between the dual tubes at the manifold splitter, flow continues through the flow tubes until it reaches the outlet splitter, and the flow is recombined back into the pipeline. Additional transducers are placed on the flow tubes to induce vibration (drive coil) which is commonly done at the geometric center of the flow tubes. There are also two sensing transducers (pickoff coils) located on the flow tube that are used to measure the frequency of vibration as well as the phase delay; these two measured variables are directly related to the fluid density and the fluid mass flow respectively. A RTD is also placed on the meter to compensate for structural changes with temperature.

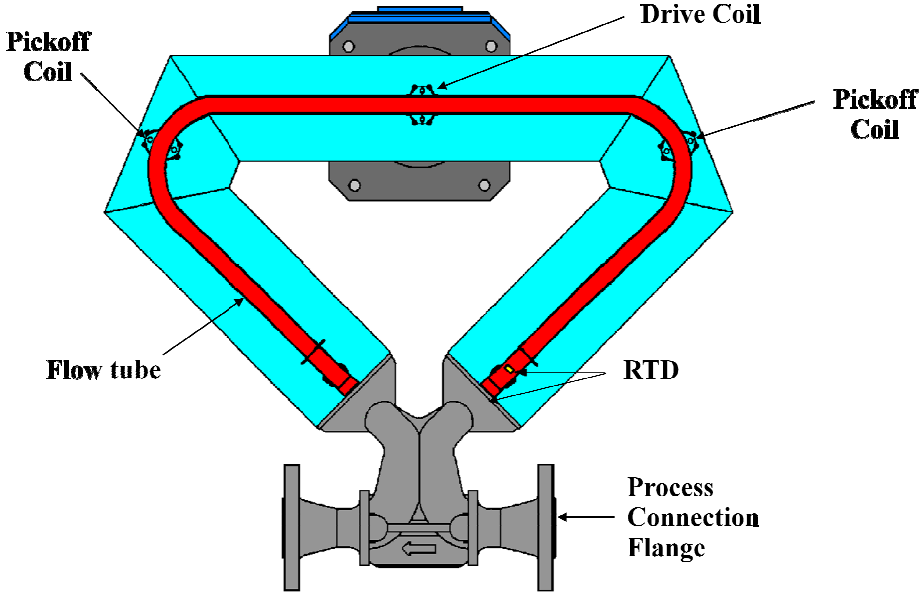

Figure 21 Coriolis Schematic

Vibration in a Coriolis meter is induced by a magnet and coil transducer where the force is proportional to current, coil wire length, and the transverse magnetic field. The vibrating system is driven at its natural frequency and a control scheme is used to limit amplitude such that the stress level in the flow tube(s) is well below the endurance limit, thus ensuring infinite life. A model for a Coriolis meter measuring density is shown below and it is important to note that this density measurement can be made with or without flow.

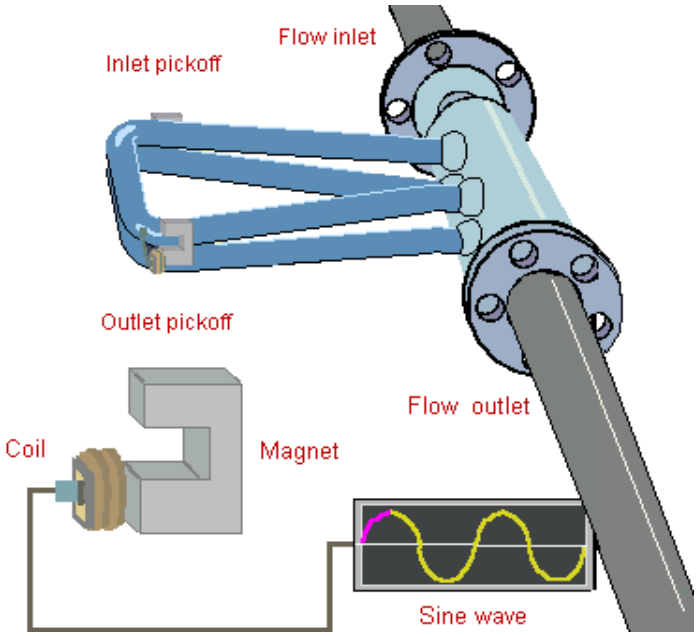

Figure 22 Coriolis Density Model

When the system is vibrated on resonance, the governing equation for the frequency of vibration (*f*) is:

$$f = \sqrt{\frac{K}{M}} = \sqrt{\frac{K}{M_T + M_F}} = \sqrt{\frac{K}{M_T + V * \rho_F}} \quad (3)$$

In this equation, the following variables are defined:

K = Stiffness of the flow tube(s)
M = Total Mass = Mass Tube + Mass Fluid = $M_T + M_F$
Mass Fluid = Volume * Density Fluid * = V * ρ_F

When the fluid density is zero the frequency reaches a maximum. As the density of the fluid increases, the frequency decreases. This relationship is used to calculate the actual density of the fluid in the flow tubes. The stiffness and geometry of the flow tubes change with temperature and are compensated using internal RTD. It is also important to note that without flow, the two sensing transducers at the inlet and outlet are in phase and at the resonant frequency.

When erosion occurs, multiple variables in the above equation are altered. As the wall of the flow tube erodes, the stiffness of the flow tube decreases producing a lower frequency reading at constant density. The mass of the flow tube also decreases creating an opposing effect at constant density, e.g. frequency increases at constant density as M_T decreases. Finally, the internal volume of the flow tube increases and more fluid participates in the vibration changing the sensitivity of the frequency-to-density relationship. Since multiple variables in the equation are affected, the measured density could be high, low, or accurate depending on the situation. Direct measurement of the tube stiffness is also useful and will be discussed in an upcoming section.

Mass flow is made using the vibrating tube device where Coriolis forces are exploited to make a mass flow measurement. These Coriolis forces produce twisting motion of the flow tube superimposed on the base vibration when flow is present. This superposition produces a vibration pattern where the inlet and outlet sensors are no longer in phase and the delay produced is directly proportional to mass flow. The figure below shows the vibration pattern with and without flow.

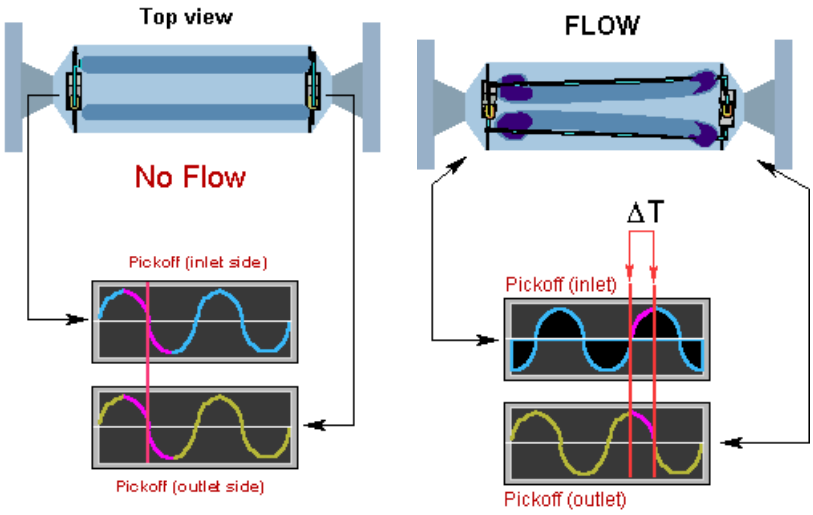

Figure 23 Coriolis Mass Flow Description

When the fluid mass flow is zero the phase delay also goes to zero. As the mass flow of the fluid increases, the phase delay increases. This relationship is used to calculate the actual mass flow of the fluid in the flow tubes. The RTD is again used to compensate for changes in stiffness and geometry. The stiffness of the flow tubes and the mass flow rate in the flow tubes are important parameters in determining mass flow.

When erosion occurs, the stiffness of the flow tubes is reduced, thus affecting the mass flow measurement. The internal volume of the flow tube increases and more fluid participates in the vibration changing the sensitivity of the phase to mass flow relationship. Since erosion can be non-uniform and different between the inlet and outlet, the geometrical changes can also create phase that is not related to mass flow. Again, since multiple variables are affected, the measured mass flow could be high, low, or accurate depending on the situation.

Although the effects from erosion on the Coriolis meter are interesting and important for measurement, the actual pressure rating and ability to contain the process fluid is of upmost importance. Coriolis meters are designed per internationally recognized pressure standards when they are designed and fabricated. A common design requirement is 100 bar rating which requires adherence to code using approved metals, approved welding practices, minimum wall thickness, along with many other requirements. When erosion occurs in a Coriolis meter and wall thicknesses diminish, the ability to hold pressure declines. As wall thickness declines, the stiffness of the flow tube also declines if erosion occurs where strain is present in the flow tubes. Thus, the ability to predict erosion, properly size meters in potentially abrasive service, provide input on preventative maintenance, recalibration intervals, and replacement plans is crucial.

7 FININTE ELEMENT ANALYSIS AND RESULTS

Vibration analysis is critical for Coriolis meter design and operation. Structural finite elements are used to model a Coriolis meter to account for complexities in geometry and to include the fluid in the analysis; both flowing and non-flowing conditions can be analyzed. In the simplest form, finite elements are simple geometric structures where the inputs and outputs are understood and can be combined together to form complicated structures. Matrix manipulation is used to solve for the outputs on these complicated structures. In addition, fluid elements can be defined and added into the structural model to solve for frequency and phase which are connected back to the fluid density and fluid mass flow. The basic matrix equation that is solved by the program is as follows where the matrix dimensions can be on the order of 10^6 or larger:

$$[M_F + M_T]\{\ddot{x}\} + [C_F + C_T]\{\dot{x}\} + [K_T]\{x\} = \{\overrightarrow{f_T} + \overrightarrow{f_F}\} \quad (4)$$

Where:

M_F = Mass Matrix of the Fluid
M_T = Mass Matrix of the Tube
C_F = Damping Matrix of the Fluid
C_T = Damping Matrix of the Tube
K_T = Stiffness Matrix of the Tube
f_T = Force vector on the tube
f_F = Force vector on the tube from the Fluid
x = position vector where each entry is defined by the node and position direction
$\dot{x}$ = velocity vector
$\ddot{x}$ = acceleration vector

To perform the analysis on the CMF300 and F300 meters, detailed tube geometries were imported from solid models. These geometries were then discretized using appropriate finite elements with particular emphasis on the wetted path so that the metal could be eroded with the defined erosion pattern. Baseline conditions were solved for each meter and the results, which include density and mass flow calibration constants, were verified against current production meters.

Based on the erosion patterns from sand in water, the erosion pattern was input to the finite element model. The individual specific elements were reduced in thickness by moving the fluid facing surface away from the fluid, thus creating a thinner flow tube. This was done across thousands of elements. Furthermore, the distance of the move was parameterized such that total erosion could be carried out in steps. A picture of each tube model with the erosion pattern present is shown below.

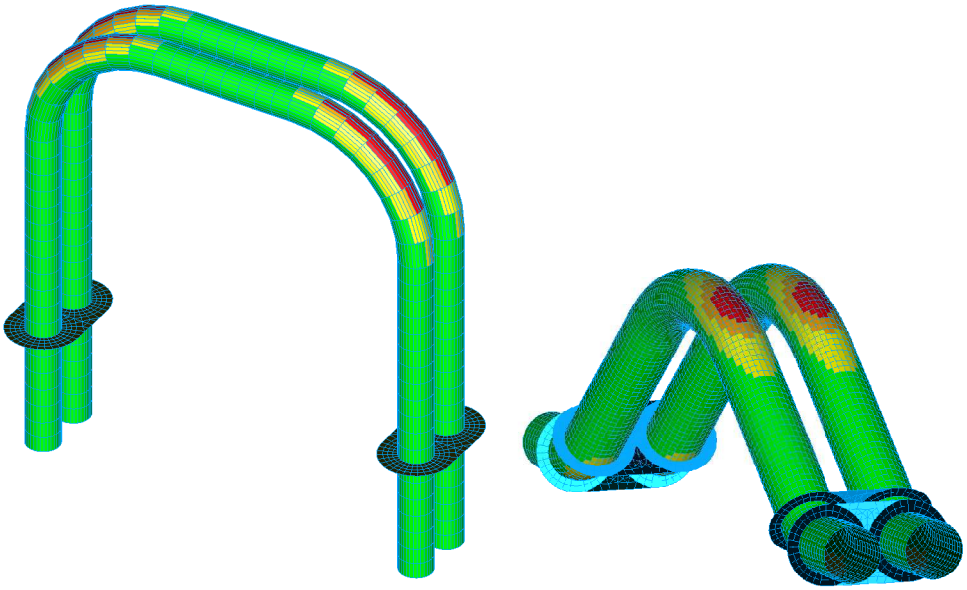

Figure 24 Erosion Patterns Modelled on CMF300 and F300

For each of these models, a common pipeline flow rate was used to define the erosion pattern at 10 m/s flow velocity in the 80mm (3 inch) pipeline. For the CMF300, 4.5e-5 mm/(kg sand) is used and 75% of wall was removed at the maximum. For the F300, 1.2e-4 mm/(kg sand) is used again to a maximum of 75% wall removal. The increased erosion in the F300 is due to the increased tube velocity (smaller flow tube and 23% higher velocity) and due to geometry based on the 45^o impingement angle. The change in calculated pressure rating based on international standards of the flow tube (listed component) is shown in Figure 25 based on percentage tube wall erosion.

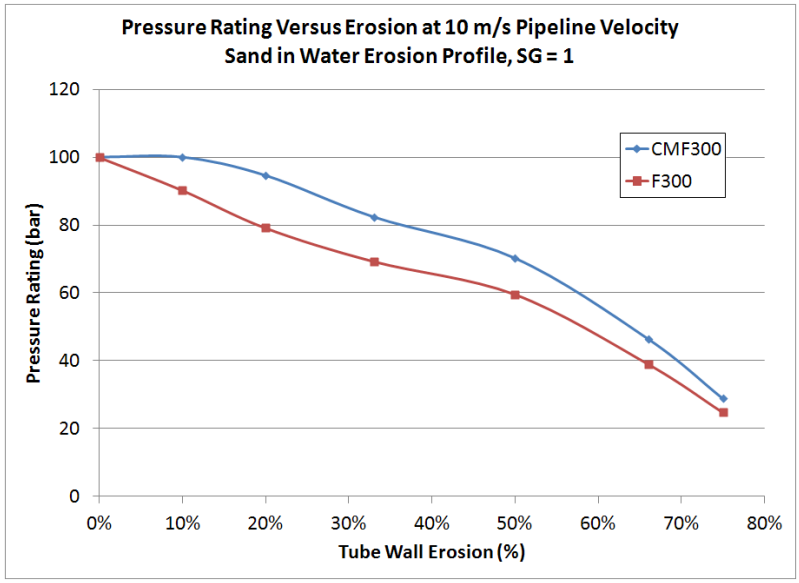

Figure 25 Pressure Rating Change versus Tube Wall Erosion

Assuming a sand rate of 5,000 kg/year (570 grams sand / hour) at a flow velocity of 10 m/s in the supply pipeline, percentage tube wall erosion can be converted into time units. The graph of pressure rating versus time is shown in Figure 26.

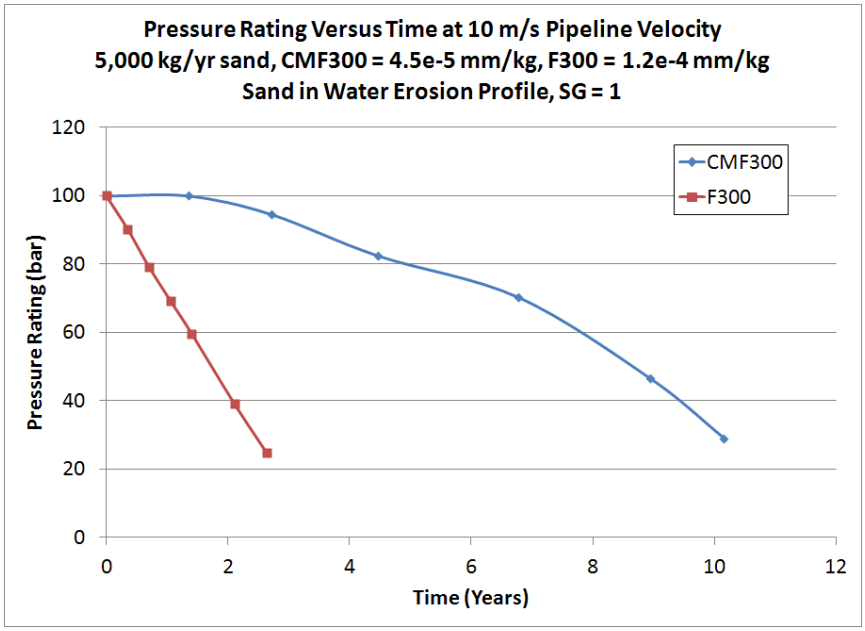

Figure 26 3" (DN75) Flow Tube Pressure Rating versus Time

Keeping constant flow rate in the supply pipeline, the F300 erodes at approximately a five times higher rate. This fact emphasizes the need to properly size and select flow meters in erosive service to provide the lowest flow velocity in the measurement tubes as well as providing the lowest Reynolds's number in the flow tubes. This result is also counter intuitive, as one might expect the lower profile meter to have superior erosion resistance.

Mass Flow Errors can be predicted using the erosion pattern versus time based on Finite Element Modelling. Figure 28 shows the Mass Flow Error versus time.

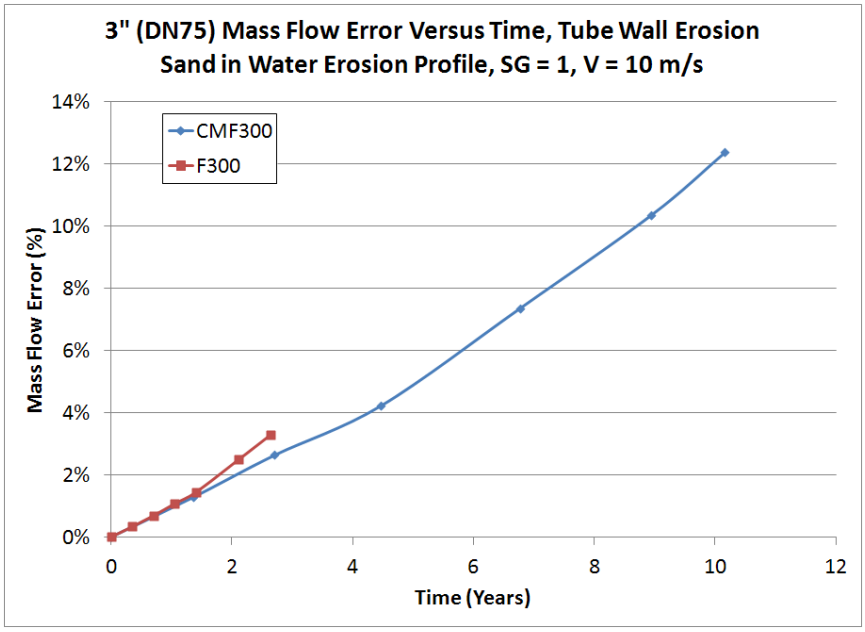

Figure 27 3" (DN75) Mass Flow Error versus Time

Figure 27 shows that both meters mass error versus time are similar, although the F300 is eroding at a much higher rate. This graph also shows that errors in mass flow, with the supplied erosion pattern for sand in water, are much lower than might be expected. Bear in mind that each graph ends with 75% of the tube wall eroded; corresponding to a 4x drop in pressure rating, and the mass flow errors are 4% and 12% for the F300 and CMF300 respectively.

Figure 28 shows the change in density error versus time for the sand in water erosion pattern with a baseline fluid density with SG = 1. Both sensors show small changes in density error which makes density field checks less useful as an indication of erosion. This is especially true using the F300 slightly curved tube geometry.

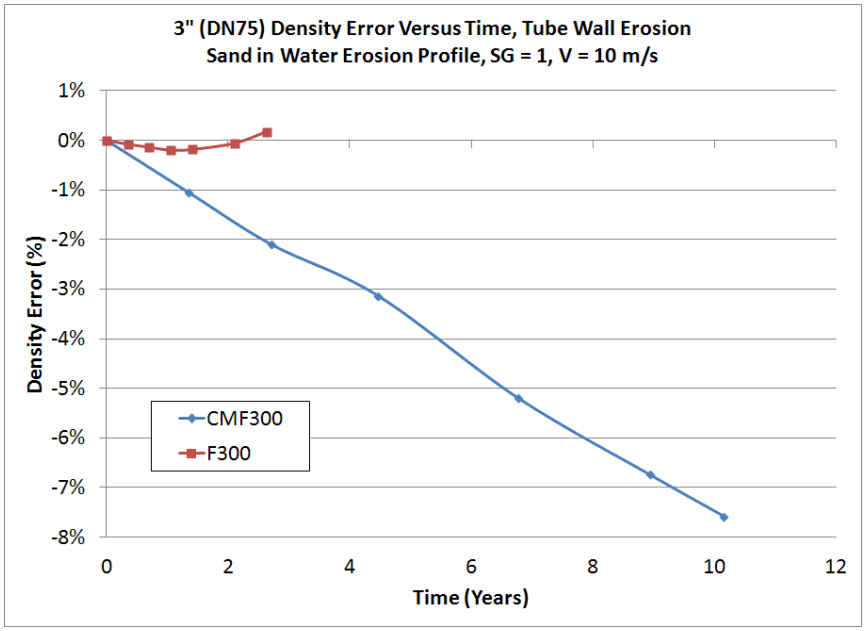

Figure 28 3" (DN75) Density Error versus Time

The volume flow errors are calculated at an SG of 1 and are the division of the mass flow and density errors. This data is shown in Figure 29.

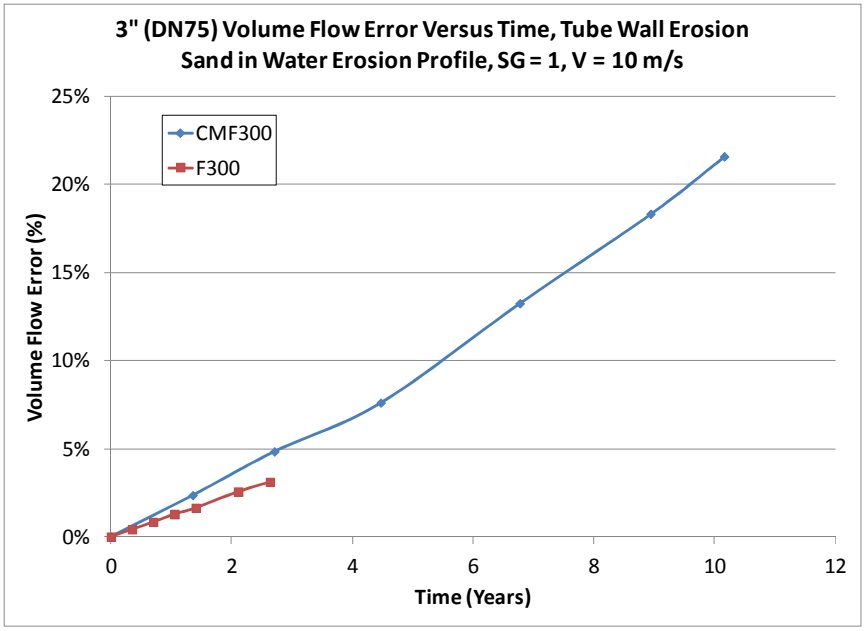

Figure 29 3" (DN75) Volume Flow Error versus Time

For the water in sand erosion pattern at 10 m/s inlet velocity after a two year time period, the results in each variable are summarized in Table 5. This table shows the importance of lower velocity, i.e. larger tube diameter, above all other parameters.

TABLE 5 - COMPARISON OF EROSION RESULTS WATER IN SAND EROSION AT 2 YEARS AT 10 M/S SUPPLY VELOCITY

	CMF300	F300
Erosion Rate (mm/kg)	4.5e-5	1.2e-4
Sand Rate (kg/year)	5,000	5,000
Tube Diameter (mm)	44.7	40.2
Flow Tube Velocity (m/s)	15.2	18.8
Erosion at 2 Years (% of Wall)	15%	59%
Pressure Rating at 2 Years (bar)	96	40
Mass Flow Error at 2 Years (%)	2.0%	2.4%
Density Error at 2 Years (% at 1000 kg/m^3)	-1.7%	-0.1%
Max Volume Error (% at 1000 kg/m^3)	3.7%	2.5%

8 CONCLUSION

Computational Fluid Dynamics (CFD) simulation was used to assess particulate erosion in two of Emerson's Micro Motion Coriolis flow meters, namely the F300 and CMF300 meters with two distinct geometries.

In water flow, CFD predicted failure to occur in the bends of the Coriolis meter tubes. In gas flow, failure was predicted to occur at the bend immediately upstream of the outlet manifold.

Certain fluid variables were investigated to see how they affected the erosion rate in the meters. These included fluid velocity, particle diameter, fluid viscosity, and installation effects. Erosion rates increased as fluid velocity increased and as viscosity decreased. The predicted erosion rate was not affected by variations in particle size although in practice particles smaller than 100 microns are likely to be less erosive.

The DNV RPO501 equation was in good agreement with the CFD results in most of the modelled cases. An equation given in DNV RPO501 can be used as a good estimate of erosion in the bends of the Coriolis meter which can be used to estimate erosion rates and pressure ratings versus time.

The effect on mass flow accuracy, density accuracy, and volume flow accuracy can be modelled using finite element methods and the DNV estimation can be used to better quantify the effects of erosion on Coriolis meters. The most important parameter is erosion rate which is higher for the F300, the dual slightly curved meter, because of geometry and the fact that the tube diameter is smaller thus the tube velocity is higher.

9 REFERENCES

[1] McLaury, B.S., Shirazi, S.A., Shadley, J.R. & Rybicki, E.F.. Parameters affecting flow accelerated erosion and erosion-corrosion, Corrosion95, NACE International Annual Conference and Corrosion Show, paper 120.

[2] Toda, M., Kamori, N., Sait, S. & Maeda, S.. Hydraulic Conveying of Solids through Pipe Bend, J. Chem. Engg. Japan 5, 1971

[3] Okita, R.. Effects of Viscosity and Sand Size on Erosion Measurements and Predictions, E/CRC November 2008

[4] Schallert, R. & Levy, E.. Effect of a combination of two elbows on particle roping in pneumatic conveying, Powder Technology 107, pp 226-233, 2000.

[5] Barton, N., Macleod, M., Zanker, K. & Stobie, G.. Erosion in subsea multiphase flow meters, The Americas Workshop 2011.

[6] Misra, A. & Finnie, I. On the size effect of abrasive and erosive wear, Wear 65, pp 359-373, 1981.

[7] Det Norske Veritas. Recommended practice RP O501: Erosive Wear in Piping Systems. 1996. Revision 2007. 7

[8] ANSYS Fluent Website www.fluent.com.

[9] Haugen, K., Kvernvold, O., Ronold, A. & Sandberg, R.. Sand erosion of wear-resistant materials: Erosion in choke valves, Wear 186-187, pp 179-188, 1995.